JOURNAL OF PROPULSION AND POWER
Vol. 11, No. 5, September–October 1995

Flutter Stability of a Detuned Cascade in Subsonic Compressible Flow

Scott Sawyer* and Sanford Fleeter†
Purdue University, West Lafayette, Indiana 47907

A mathematical model is developed to predict the unsteady aerodynamics of a detuned two-dimensional flat plate cascade in subsonic compressible flow. Aerodynamic detuning is introduced by nonuniform circumferential spacing and chordwise offset. Combined aerodynamic-structural detuning is accomplished by replacing alternate airfoils with splitter blades. A torsion mode stability analysis that considers aerodynamic and combined aerodynamic-structural detuning is developed by combining the unsteady aerodynamic model with a single degree-of-freedom structural model. The effect of these detuning techniques on flutter stability is then demonstrated by applying this model to a baseline unstable 12-bladed rotor and detuned variations of this rotor. This study demonstrates that detuning is a viable passive flutter control technique.

Nomenclature

A = cascade A airfoil index
a = freestream speed of sound
B = cascade B airfoil index
C_L = lift coefficient
C_M = moment coefficient
C_r = ratio of chord length of cascade B to cascade A
c_A = chord length of cascade A
c_B = chord length of cascade B
ea = elastic axis location
k = reduced frequency $\omega c/W$
n = airfoil index
os = chordwise offset of cascade B relative to cascade A
p = unsteady pressure perturbation
$\bar{p}$ = complex strength of unsteady pressure perturbation
r_α = radius of gyration
S = circumferential spacing
S_r = circumferential spacing ratio, S_0/S
S_0 = circumferential distance between adjacent cascade A and cascade B airfoils
U = freestream axial velocity
u = unsteady axial velocity perturbation
$\bar{u}$ = complex strength of axial velocity perturbation
V = freestream tangential velocity
v = unsteady tangential velocity perturbation
$\bar{v}$ = complex strength of tangential velocity perturbation
W = freestream flow velocity
w = upwash normal to the airfoil
x = axial coordinate
y = tangential coordinate
z = chordwise coordinate
α = axial wave number
β = tangential wave number
Γ = bound vortex distribution
δ = bound vortex distribution curve-fit coefficients
μ = nondimensional mass ratio
ρ = unsteady density perturbation
$\bar{\rho}$ = complex strength of unsteady density perturbation
ρ_0 = freestream density
σ = interblade phase angle
ψ = stagger angle
ω = circular frequency
ω_n = airfoil natural frequency

Presented as Paper 94-0144 at the AIAA 32nd Aerospace Sciences Meeting and Exhibit, Reno, NV, Jan. 10–13, 1994; received Jan. 28, 1994; revision received Oct. 17, 1994; accepted for publication Oct. 24, 1994.

*AFRAPT Trainee, School of Mechanical Engineering. Student Member AIAA.
†Professor, School of Mechanical Engineering. Associate Fellow AIAA.

Introduction

VARIOUS techniques are being considered for aeroelastic control of advanced design turbomachine blade rows. Structural detuning, defined as designed blade-to-blade differences in the natural frequencies of a blade row, is a passive aeroelastic control technique. Analyses have been developed that show that structural detuning is beneficial with regard to flutter, with alternate blade structural detuning optimal.[1] However, structural detuning is not universally accepted as a passive aeroelastic control concept due to the associated manufacturing material, inventory, and cost problems.

Aerodynamic detuning is a relatively new concept for passive aeroelastic control. Aerodynamic detuning is defined as designed blade-to-blade differences in the unsteady aerodynamic flowfield of a blade row, thereby resulting in blade-to-blade differences in the unsteady aerodynamic forces and moments. These differences affect the fundamental driving force of flutter, the unsteady aerodynamic loading on the blade. This results in the blading not responding in a classical traveling wave mode typical of a conventional uniformly spaced tuned rotor. Studies of rotors operating in both incompressible flowfields[2,3] and supersonic flowfields[4,5] have shown that aerodynamic detuning is beneficial to flutter stability.

Combined aerodynamic-structural detuning incorporates blade-to-blade differences in both the blade unsteady aerodynamics and structural properties, i.e., the blade natural frequencies. One particular concept for this combined detuning involves inserting splitters or short chord airfoils into adjacent passages of a rotor. The splitters have a higher natural frequency and different unsteady aerodynamics than the adjacent full chord airfoils. Incorporating splitters into a rotor design to introduce combined aerodynamic-structural detuning for passive aeroelastic control has been considered for rotors operating in either an incompressible or a supersonic flow.[2,3,6,7]

In this article, a mathematical model is developed to analyze the unsteady aerodynamics of a detuned flat plate airfoil cascade in a compressible subsonic flow generated by harmonic torsion mode airfoil oscillations. The linearized two-dimensional continuity and momentum equations for inviscid isentropic compressible flow are solved using wave theory, a

technique first utilized for a uniformly spaced airfoil cascade.[8] This technique is extended herein to analyze detuned airfoil cascades made up of alternate nonuniformly spaced airfoils with different chord lengths, elastic axis locations, and chordwise offset positions. The detuned cascade is constructed by the superposition of two uniformly spaced or conventional tuned cascades. The solution of the governing equations yields the airfoil unsteady bound vortex distribution that is equivalent to the airfoil unsteady pressure distribution and determines the unsteady aerodynamic loading. The torsion mode stability of the cascade is then analyzed by combining the unsteady aerodynamic loading with a single degree-of-freedom structural model. The effects of the detuning parameters on flutter are then demonstrated.

Unsteady Aerodynamic Model

To analyze the unsteady aerodynamics of an aerodynamically detuned cascade, it is necessary to develop an understanding of the fundamentals of two-dimensional subsonic compressible inviscid flow as applied to a uniformly spaced or tuned cascade. This tuned cascade analysis is then extended to the detuned cascade.

Figure 1 shows a conventional uniformly spaced tuned cascade with $n = 0$ denoting the reference airfoil. The upwash on the cascaded airfoils relative to the reference airfoil is determined by the interblade phase angle σ, i.e., the upwash on airfoil $n = 1$ is the upwash on the zeroth airfoil multiplied by $e^{i\sigma}$.

An aerodynamically detuned cascade is depicted in Fig. 2. It is the combination of two uniformly spaced tuned cascades, denoted as cascade A and cascade B for convenience, and identified by the indices A and B. These tuned cascades have the same stagger angle ψ and circumferential spacing S. The coordinate system for cascade A is (x, y, z), with the cascade B coordinate system (x', y', z'). Note that z and z', the chordwise coordinates, are not orthogonal to the axial and tangential coordinates (x, y) or (x', y'). The origins for the cascade A and B coordinate systems are at the leading edge of the zeroth blades of each cascade. The airfoils of cascade A may have different chord lengths than those of cascade B. The airfoil chords are denoted by c_A and c_B, with the cascade A to B airfoil chord ratio defined as $C_r = c_A/c_B$. Additional parameters to define the detuned cascade geometry include the following. The tangential distance between adjacent cascade A and B airfoils in the detuned cascade is S_0. The cascade A to cascade B airfoil spacing ratio is $S_r = S_0/S$. The chordwise offset os is the distance in the z direction from the stagger line of cascade A to the stagger line of cascade B. A tuned cascade thus corresponds to a detuned cascade when $\sigma_{\text{detuned}} = 2\sigma_{\text{tuned}}$, $S_{\text{detuned}} = 2S_{\text{tuned}}$, $S_r = 0.5$, $C_r = 1.0$, and $os = 0.0$.

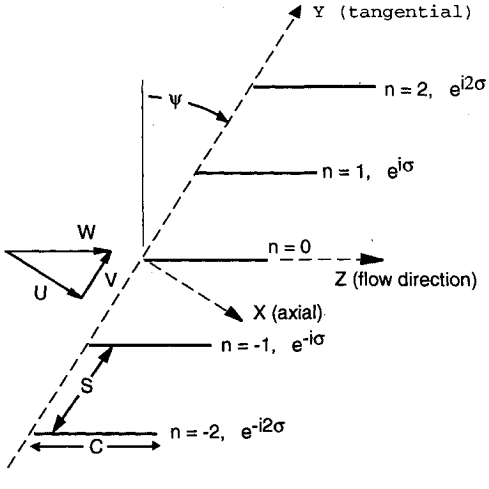

Fig. 1 Tuned cascade geometry.

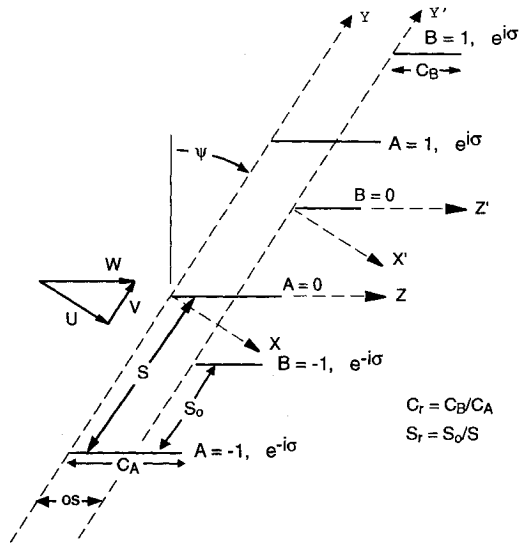

Fig. 2 Detuned cascade geometry.

Plane Wave Solutions of the Linearized Euler Equations

The two-dimensional inviscid compressible flow continuity and momentum equations linearized about a uniform mean flow are given in Eq. (1):

$$\begin{aligned} &\frac{\partial \rho}{\partial t} + U\frac{\partial \rho}{\partial x} + V\frac{\partial \rho}{\partial y} + \rho_0\left(\frac{\partial u}{\partial x} + \frac{\partial v}{\partial y}\right) = 0 \\ &\frac{\partial u}{\partial t} + U\frac{\partial u}{\partial x} + V\frac{\partial u}{\partial y} + \frac{1}{\rho_0}\frac{\partial p}{\partial x} = 0 \\ &\frac{\partial v}{\partial t} + U\frac{\partial v}{\partial x} + V\frac{\partial v}{\partial y} + \frac{1}{\rho_0}\frac{\partial p}{\partial y} = 0 \end{aligned} \tag{1}$$

where U and V are the steady freestream velocities in the axial and tangential (x, y) directions, u and v are the corresponding unsteady perturbation velocity components, ρ_0 and ρ are the freestream and perturbation densities, and the perturbation pressure is p.

The velocity and pressure perturbations are assumed to be harmonic in time and space:

$$\begin{bmatrix} u \\ v \\ p \end{bmatrix} = \begin{bmatrix} \bar{u} \\ \bar{v} \\ \bar{p} \end{bmatrix} \exp[i(\omega t + \alpha x + \beta y)] \tag{2}$$

where $\bar{u}$, $\bar{v}$, and $\bar{p}$ are complex constants specifying the magnitude of the perturbation velocities and pressure, α and β are the axial and tangential wave numbers, and ω is the frequency.

The pressure and density perturbations are related through the isentropic flow relation $\partial p/\partial \rho_{|s} = a^2$, where a is the speed of sound. Hence,

$$\bar{p} = a^2\bar{\rho} \tag{3}$$

Substituting Eqs. (2) and (3) into the linearized continuity and momentum equations leads to the following system of homogeneous algebraic equations:

$$\begin{bmatrix} (\omega + U\alpha + V\beta) & a^2\alpha\rho_0 & a^2\beta\rho_0 \\ \alpha/\rho_0 & (\omega + U\alpha + V\beta) & 0 \\ \beta/\rho_0 & 0 & (\omega + U\alpha + V\beta) \end{bmatrix} \times \begin{bmatrix} \bar{p} \\ \bar{u} \\ \bar{v} \end{bmatrix} = 0 \tag{4}$$

For a nontrivial solution, the determinant of the coefficients must be zero. Expanding this determinant leads to the following characteristic equation, which has two families of solutions:

$$[(\omega + \alpha U + \beta V)^2 - a^2(\alpha^2 + \beta^2)][\omega + \alpha U + \beta V] = 0 \tag{5}$$

When $[\omega + \alpha U + \beta V] = 0$, the solution corresponds to vorticity waves that are simply convected with the mean flow, with no associated pressure perturbations. The axial wave number α for this vorticity wave solution is

$$\alpha = [(\omega + V\beta)/U] \tag{6}$$

The solution family for the case when $[(\omega + \alpha U + \beta V)^2 - a^2(\alpha^2 + \beta^2)] = 0$ corresponds to a pair of irrotational pressure waves, with one propagating upstream and the other downstream at the speed of sound. The axial wave numbers α for these pressure waves are

$$\alpha = \frac{U(\omega + V\beta) \pm a\sqrt{(\omega + V\beta)^2 - (a^2 - U^2)\beta^2}}{a^2 - U^2} \tag{7}$$

The propagation of the unsteady pressure perturbations, described by the values of α, depend on the values of the arguments under the radical. Three possibilities exist.

If $(\omega + V\beta)^2 - (a^2 - U^2)\beta^2 = 0$, there is one axial wave number that is real. Only one wave is created that propagates in the tangential direction. This is an acoustic resonance condition also known as cutoff. When $(\omega + V\beta)^2 - (a^2 - U^2)\beta^2 > 0$, two waves propagate without decay, one going upstream and the other downstream. This behavior is termed superresonant for a subsonic mean flowfield. The case with $(\omega + V\beta)^2 - (a^2 - U^2)\beta^2 < 0$ is termed subresonant and the waves decay exponentially with axial distance.

The unsteady aerodynamic loading on the blading is modeled by replacing the airfoils with bound vortex sheets. The vorticity distribution is then expanded in a Fourier series in the tangential direction, with the various harmonics specified by the index r. Unsteady cascade periodicity requirements then specify β

$$\beta = (\sigma - 2\pi r)/S, \qquad r = 0, \pm 1, \pm 2, L \tag{8}$$

where r is the mode number.

Tuned Cascade Kernel Function

The airfoil surface boundary condition specifies the normal velocity component, i.e., the upwash. Thus, it is necessary to determine the bound vortex distribution that satisfies the specified upwash distribution. This is accomplished by determining an integral equation that relates the bound vortex distribution to the upwash specified at a particular point.

Determined by the three solutions determined previously, a bound vortex row produces three waves, upstream and downstream going pressure waves and a downstream going vorticity wave. As defined, the bound vorticity is zero off the blade and proportional to the unsteady surface pressure differential.

The upwash at a particular point on the reference airfoil is given by the velocity perturbation in the tangential and axial directions. The upwash on the airfoil upstream of a bound vortex row due to the upstream going pressure wave is

$$w(z) = \frac{\Gamma(z_0)}{S} \sum_{r=-\infty}^{\infty} \bar{w}_1 \exp[i(\alpha_1 \Delta x + \beta \Delta y)] \tag{9}$$

where (x, y) and (x_0, y_0) are the locations of the upwash and the vortex on the reference airfoil, respectively, $\bar{w}_1$ is the complex magnitude of the disturbance caused by an upstream going pressure wave as given by Smith,[8] w is the specified upwash perpendicular to the chordwise axis, $\Delta x = x - x_0 < 0$ and $\Delta y = y - y_0 < 0$ are the components of the distance from the location of the vortex (x_0, y_0) to the location where the upwash is specified (x, y) (Fig. 3). Note that the specification of Δx and Δy is the key point in the development of the kernel function for the detuned cascade.

The upwash downstream of the vortex row, with both the downstream going pressure wave and the convected vorticity wave, is

$$w(z) = \frac{\Gamma(z_0)}{S} \sum_{r=-\infty}^{\infty} \{\bar{w}_2 \exp[i(\alpha_2 \Delta x + \beta \Delta y)] + \bar{w}_3 \exp[i(\alpha_3 \Delta x + \beta \Delta y)]\} \tag{10}$$

where $\bar{w}_2$ and $\bar{w}_3$ are complex magnitudes for the disturbance caused by a downstream going pressure and vorticity waves as given by Smith.[8]

Equations (9) and (10) are valid for a single vortex row. To determine the upwash due to a vortex distribution along the airfoil chord, these equations are integrated over the airfoil chord:

$$w(z) = \int_0^z \left\{ \frac{\Gamma(z_0)}{S} \sum_{r=-\infty}^{\infty} \bar{w}_2 \exp[i(\alpha_2 \Delta x + \beta \Delta y)] + \sum_{r=-\infty}^{\infty} \bar{w}_3 \exp[i(\alpha_3 \Delta x + \beta \Delta y)] \right\} dz_0 + \int_z^c \frac{\Gamma(z_0)}{S} \sum_{r=-\infty}^{\infty} \bar{w}_1 \exp[i(\alpha_1 \Delta x + \beta \Delta y)]\, dz_0 \tag{11}$$

where z_0 is the chordwise vortex location, and z is the chordwise upwash location (Fig. 3).

The kernel function is defined such that

$$w(z) = \int_0^1 \Gamma(z_0) K(\Delta x, \Delta y)\, dz_0 \tag{12}$$

Comparing Eqs. (11) and (12), the kernel function is

$$K = \frac{c}{S} \begin{cases} \sum_{r=-\infty}^{\infty} \bar{w}_2 \exp[i(\alpha_2 \Delta x + \beta \Delta y)] + \sum_{r=-\infty}^{\infty} \bar{w}_3 \exp[i(\alpha_3 \Delta x + \beta \Delta y)] & z_0 < z \\ \sum_{r=-\infty}^{\infty} \bar{w}_1 \exp[i(\alpha_1 \Delta x + \beta \Delta y)] & z_0 > z \end{cases} \tag{13}$$

Specifying the upwash $w(z)$, and calculating the kernel function, Eq. (12) can be solved for $\Gamma(z_0)$, which is related to the unsteady pressure differences across the airfoil chord line.

The solution for the unsteady bound vorticity distribution is found by the method of collocation and matrix inversion subject to the Kutta condition at the trailing edge using standard methods.

Aerodynamically Detuned Cascade Kernel Function

The kernel functions derived for the tuned cascade are applied to aerodynamically detuned cascades. This is accomplished through the geometric factors Δx and Δy. Namely, the values of Δx and Δy are determined by the spacing ratio, the chord ratio, and the offset that specify the detuned cascade geometry.

The geometric factors Δx and Δy become more complicated for a detuned cascade, but are found in the same manner as

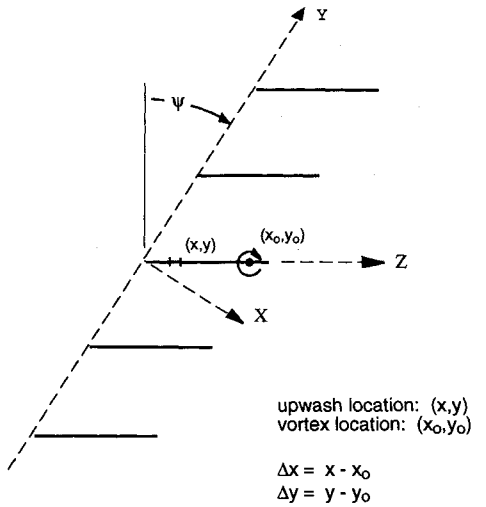

Fig. 3 Tuned cascade with vortex at (x_0, y_0) and upwash specified at (x, y).

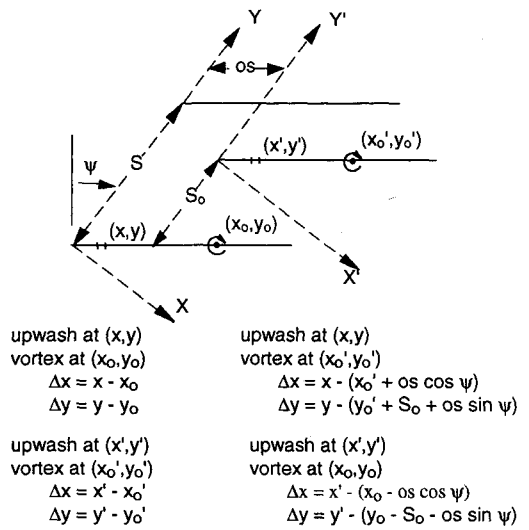

Fig. 4 Detuned cascade showing possible upwash and vortex location combinations.

for the tuned cascade (Fig. 4). The upwash is specified at location (x, y). For the vortex located at (x_0, y_0) on cascade A, Δx and Δy take the form $\Delta x = x - x_0$ and $\Delta y = y - y_0$ for upwash at (x, y) on cascade A, and $\Delta x = x' - (x_0 - os \cos \psi)$ and $\Delta y = y' - (y_0 - S_0 - os \sin \psi)$ for upwash at (x', y') on cascade B. Similarly for the vortex located at (x_0', y_0') on cascade B, Δx and Δy take the form $\Delta x = x' - x_0'$ and $\Delta y = y' - y_0'$ for upwash at (x', y') on cascade B, and $\Delta x = x - (x_0' + os \cos \psi)$ and $\Delta y = y - (y_0' + S_0 + os \sin \psi)$ for upwash at (x, y) on cascade A. These factors must be specified for each case: the upwash specified on cascade A with a vortex on cascade A or cascade B given by kernel functions K_{AA} and K_{BA}, respectively, and the upwash specified on cascade B with a vortex on cascade A or cascade B given by kernel functions K_{AB} and K_{BB}, respectively.

The kernel functions for a detuned cascade are given below. For $z_0 < z$, the kernel function represents the downstream going pressure wave and the vorticity wave that has been replaced by an analytical expression:

$$K_{AA} = \frac{c_A}{S} \sum_{r=-\infty}^{\infty} \bar{w}_2 \exp\{i[\alpha_2(x - x_0) + \beta(y - y_0)]\}$$

$$+ \frac{c_A}{S}\frac{k}{2} \frac{\sinh\left(k \frac{S}{c_A} \cos\psi\right) e^{-ik(z-z_0)}}{\cosh\left(k \frac{S}{c_A} \cos\psi\right) - \cos\left(\sigma + k \frac{S}{c_A} si\psi\right)}$$

$$K_{BA} = \frac{c_B}{S} \sum_{r=-\infty}^{\infty} \bar{w}_2 \exp(i\{\alpha_2[x - (x_0' + os \cos\psi)]$$

$$+ \beta[y - (y_0' + S_0 + os \sin\psi)]\})$$

$$- \frac{c_B}{S}\frac{ik}{4} \exp\left\{i\left[-k(z' - z_0) - \frac{kos}{c_B} + \sigma\frac{S_0}{S}\right]\right\}$$

$$\times \left\{\frac{\exp\left[-ir_2\pi\left(1 - 2\frac{S_0}{S}\right)\right]}{\sin \pi r_2} - \frac{\exp\left[-ir_1\pi\left(1 - 2\frac{S_0}{S}\right)\right]}{\sin \pi r_1}\right\}$$

$$K_{BB} = \frac{c_B}{S} \sum_{r=-\infty}^{\infty} \bar{w}_2 \exp\{i[\alpha_2(x' - x_0') + \beta(y' - y_0')]\}$$

$$+ \frac{c_B}{S}\frac{k}{2} \frac{\sinh\left(k \frac{S}{c_B} \cos\psi\right) e^{-ik(z'-z_0')}}{\cosh\left(k \frac{S}{c_B} \cos\psi\right) - \cos\left(\sigma + k \frac{S}{c_B} \sin\psi\right)}$$

$$K_{AB} = \frac{c_A}{S} \sum_{r=-\infty}^{\infty} \bar{w}_2 \exp(i\{\alpha_2[x' - (x_0 - os \cos\psi)]$$

$$+ \beta[y' - (y_0 - S_0 - os \sin\psi)]\})$$

$$+ \frac{c_A}{S}\frac{ik}{4\pi} \exp\left\{i\left[-k(z' - z_0) - \frac{kos}{c_A} + \sigma\frac{S_0}{S}\right]\right\}$$

$$\times \left\{\frac{\exp\left[-ir_2\pi\left(1 - 2\frac{S_0}{S}\right)\right]}{\sin \pi r_2} - \frac{\exp\left[-ir_1\pi\left(1 - 2\frac{S_0}{S}\right)\right]}{\sin \pi r_1}\right\} \tag{14}$$

where K_{AA} is the effect of the upwash of cascade A on cascade A, K_{BA} is the effect of the upwash of cascade A on cascade B, K_{BB} is the effect of the upwash of cascade B on cascade B, and K_{AB} is the effect of the upwash of cascade B on cascade A.

For $z_0 > z$, the kernel function represents the upstream going pressure wave

$$K_{AA} = \frac{c_A}{S} \sum_{r=-\infty}^{\infty} \bar{w}_1 \exp\{i[\alpha_1(x - x_0) + \beta(y - y_0)]\}$$

$$K_{BA} = \frac{c_B}{S} \sum_{r=-\infty}^{\infty} \bar{w}_1 \exp(i\{\alpha_1[x - (x_0' + os \cos\psi)]$$

$$+ \beta[y - (y_0' + S_0 + os \sin\psi)]\}) \tag{15}$$

$$K_{BB} = \frac{c_B}{S} \sum_{r=-\infty}^{\infty} \bar{w}_1 \exp\{i[\alpha_1(x' - x_0') + \beta(y' - y_0')]\}$$

$$K_{AB} = \frac{c_A}{S} \sum_{r=-\infty}^{\infty} \bar{w}_1 \exp(i\{\alpha_1[x' - (x_0 - os \cos\psi)]$$

$$+ \beta[y' - (y_0 - S_0 - os \sin\psi)]\})$$

where K_{AA} is the effect of the upwash of cascade A on cascade A, K_{BA} is the effect of the upwash of cascade A on cascade B, K_{BB} is the effect of the upwash of cascade B on cascade B, and K_{AB} is the effect of the upwash of cascade B on cascade A.

Solution Method

The unknown vortex distributions on cascades A and B are found by solving the upwash integral equation, analogous to the tuned cascade solution. The integral is evaluated numerically using the trapezoidal rule. A variable transformation is used to resolve the high gradients near the leading edge. This yields a linear system of equations with the upwash specified and the vortex strength unknown. A polynomial curve fit that implicitly satisfies the Kutta condition is determined to approximate the vortex strength. The coefficients of the curve fit are determined by solution of the linear system of equations. With the coefficients determined, the vortex distribution is calculated and the unsteady lift and moment coefficients are determined.

The relationship between the unknown vortex strength and the known kernel function and upwash is

$$\begin{aligned} w_A(z) &= \int_0^1 \Gamma_A(z_0)K_{AA}\,dz_0 + \int_0^{c_r} \Gamma_B(z_0)K_{BA}\,dz_0 \\ w_B(z) &= \int_0^1 \Gamma_A(z_0)K_{AB}\,dz_0 + \int_0^{c_r} \Gamma_B(z_0)K_{BB}\,dz_0 \end{aligned} \tag{16}$$

Consider the general case where

$$w(z) = \int_0^1 \Gamma(z_0)K(\Delta x, \Delta y)\,dz_0 \tag{17}$$

To improve the accuracy of the numerical integration by better handling the high gradients near the leading edge, a transformation from the (z, z_0) domain to the (ϕ, θ) domain is utilized. Transforming Eq. (17) and evaluating the integral using the trapezoidal rule leads to

$$w(z_i) = \frac{\pi}{2n} \sum_{j=0}^{n}{}' \sqrt{\frac{1 - z_{0j}}{z_{0j}}} \left[\sum_{l=0}^{n-1} \delta_l (z_{0j})^l \right] K(\Delta x, \Delta y)_{i,j} \sin \theta_j$$

where

$$z_i = \frac{1}{2}(1 - \cos \phi_i), \quad \phi_i = \frac{\pi(2i - 1)}{2n}, \quad i = 1, 2, L\, n$$

$$z_j = \frac{1}{2}(1 - \cos \theta_j), \quad \theta_j = \frac{\pi j}{n}, \quad j = 0, 1, L\, n$$

$$\Gamma(z_0) = \sqrt{\frac{1 - z_{0j}}{z_{0j}}} \sum_{l=0}^{n-1} \delta_l (z_{0j})^l$$

Note that at the trailing edge $\Gamma(1) = 0$. Thus, the Kutta condition is implicitly satisfied.

In matrix form this equation is

$$[w_i] = \begin{bmatrix} c_{11} & L & c_{1n} \\ M & c_{im} & M \\ c_{n1} & L & c_{nn} \end{bmatrix} \begin{bmatrix} \delta_1 \\ M \\ \delta_n \end{bmatrix} \tag{18}$$

where

$$c_{im} = \frac{\pi}{2n} \sum_{j=0}^{n-1}{}' \sqrt{\frac{1 - z_{0j}}{z_{0j}}} (z_{0j})^{m-1} K(\Delta x, \Delta y)_{i,j} \sin \theta_j$$

and the unknown is now δ rather than Γ.

Extending this to the solution of the detuned cascade

$$\begin{bmatrix} [w_A] & 0 \\ 0 & [w_B] \end{bmatrix} = \begin{bmatrix} [c_{AA}] & [c_{BA}] \\ [c_{AB}] & [c_{BB}] \end{bmatrix} \begin{bmatrix} [\delta_{AA}] & [\delta_{BA}] \\ [\delta_{AB}] & [\delta_{BB}] \end{bmatrix} \tag{19}$$

where the first subscript on δ denotes which cascade oscillates or has a convected harmonic gust, with the second subscript denoting which cascade the vortex is on. For example, δ_{AB} represents the coefficients for a vortex on the reference airfoil of cascade B due to upwash on the reference airfoil of cascade A. The unsteady aerodynamics of cascades A and B are specified by means of an influence coefficient technique.

To solve the upwash integral equation, the upwash is specified to be an airfoil oscillating in torsion

$$w = W\alpha[1 + i(z - ea)k]e^{i\omega t} \tag{20}$$

where α is the magnitude of the oscillation and $k = \omega c/W$ is the reduced frequency.

The relationship between the bound vorticity and the unsteady pressure is

$$p_+ - p_- = \rho_0 W \Gamma$$

Thus, the unsteady aerodynamic lift L and moment M are

$$\begin{aligned} L &= -\rho_0 W \int_0^c \Gamma(z_0)\,dz_0 \\ M &= -\rho_0 W \int_0^c \Gamma(z_0)(z_0 - ea)\,dz_0 \end{aligned} \tag{21}$$

where ea denotes the elastic axis location.

Torsion Mode Flutter Stability

A single-degree-of-freedom model is developed for the two reference airfoils of the detuned cascade. Figure 5 shows the reference airfoils and the unsteady aerodynamic moments acting on them. The airfoil inertial properties are given by the moment of inertia about the elastic axis, with the elastic restoring forces modeled by a torsion spring acting at the elastic axis. The equations of motion, determined using Lagrange's technique, are

$$\begin{aligned} I_A \ddot{\alpha}_A + K_{SA}\alpha_A &= M_\alpha^A e^{i\omega t} \\ I_B \ddot{\alpha}_B + K_{SB}\alpha_B &= M_\alpha^B e^{i\omega t} \end{aligned} \tag{22}$$

where $I_{A,B}$ is the moment of inertia, $\ddot{\alpha}_{A,B}$ is the angular acceleration, $\alpha_{A,B}$ is the angular deflection, $K_{SA,B}$ is the torsion spring constant, and $M_\alpha^{A,B}$ represents the unsteady aerodynamic moment due to the torsional motion of the airfoils.

The unsteady aerodynamic moments are determined from the nondimensional moment coefficients, with harmonic airfoil motion considered

$$\begin{aligned} M_\alpha^A &= \pi c_A^2 \rho_0 W^2 (\alpha_A C_{M\alpha}^{AA} + \alpha_B C_{M\alpha}^{BA}) \\ M_\alpha^B &= \pi c_B^2 \rho_0 W^2 (\alpha_A C_{M\alpha}^{AB} + \alpha_B C_{M\alpha}^{BB}) \end{aligned}$$

where $\alpha_{A,B} = \bar{\alpha}_{A,B} e^{i\omega t}$.

The airfoils are modeled as cantilevered beams, thereby specifying the ratio of the natural frequencies of the cascade A and B reference airfoils. Hence, the ratio of the natural frequencies given by the chord ratio specifies the structural detuning of the cascade:

$$\omega_{nB}^2/\omega_{nA}^2 = c_A/c_B \tag{23}$$

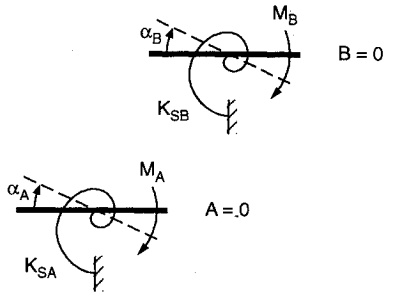

Fig. 5 Single degree-of-freedom model of detuned cascade.

The equations of motion thus become

$$\begin{bmatrix} \mu(r_\alpha k)^2\left(\frac{\omega_n^2}{\omega^2}-1\right) - C_{M\alpha}^{AA} & -C_{M\alpha}^{BA} \\ -C_{M\alpha}^{AB} & \mu(r_\alpha k C_r)^2\left(\frac{\omega_n^2}{\omega^2}-1\right) - C_{M\alpha}^{BB} \end{bmatrix} \times \begin{bmatrix} \alpha_A \\ \alpha_B \end{bmatrix} = 0$$

where

$$\mu_{A,B} = \frac{m_{A,B}}{\pi c_{A,B}^2 \rho_0}$$

is the mass ratio and

$$r_{\alpha_{A,B}} = \sqrt{\frac{I_{A,B}}{m c_{A,B}^2}}$$

is the nondimensional radius of gyration.

This matrix equation represents a standard eigenvalue problem. For a nontrivial solution, the determinant of the coefficient matrix must be zero. The determinant of the coefficient matrix is a quadratic in the square of the frequency ratio ω/ω_n. The eigenvector α_B/α_A represents the complex vibrational amplitude of cascade B relative to cascade A. The phase angle of the eigenvector represents the interblade phase angle (nominally half of the specified detuned interblade phase angle for a tuned cascade). The stability criterion requires that the real part of the exponent $i\omega$ is less than zero so that a disturbance will decay.

$$\text{real}\left(i\frac{\omega}{\omega_n}\right) < 0 \qquad \text{for stability}$$

Unsteady Aerodynamic Model Verification

The validity of this unsteady aerodynamic model is demonstrated by correlating predictions from the model developed herein to the corresponding predictions from the unsteady aerodynamic model for tuned cascades in compressible flow and detuned cascades in incompressible flow.

In general, the phase angle between the reference airfoils of cascade A and cascade B is not known. However, for a tuned cascade, the phase angle between the reference airfoils of cascade A and cascade B must be one-half the detuned interblade phase angle:

$$C_M = C_M^{AA} + C_M^{BA} e^{-i\sigma/2} \quad \text{or} \quad C_M = C_M^{AB} e^{i\sigma/2} + C_M^{BB}$$

where C_M is the tuned cascade moment coefficient, C_M^{AA}, C_M^{BA}, C_M^{AB}, and C_M^{BB} are the detuned cascade moment coefficients and σ is the detuned interblade phase angle.

The model developed by Smith[8] considers uniformly spaced tuned flat plate cascades. This is a special case of the detuned cascade model developed here, specified by $S/c = 1.0$, $M = 0.5$, $\psi = 45$ deg, $k = 0.8$ and $ea = 0.5$, with corresponding detuned cascade geometry given by $S/c = 2.0$, $C_r = 1.0$, $S_r = 0.5$, $os = 0.0$, $M = 0.5$, $\psi = 45$ deg, $k = 0.8$, and $ea_a = ea_b = 0.5$.

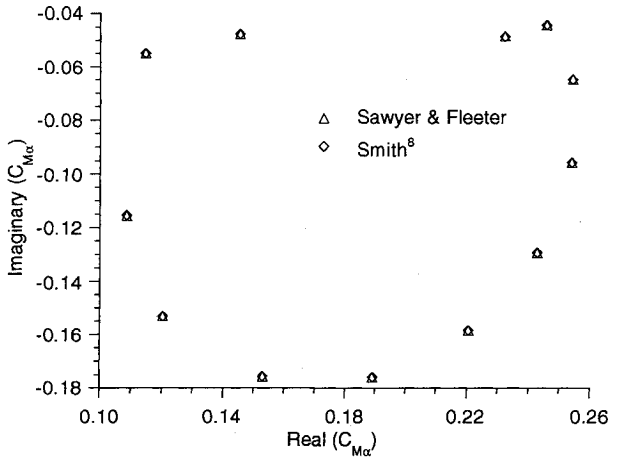

Fig. 6 Aerodynamic model verification for a tuned cascade in torsion.

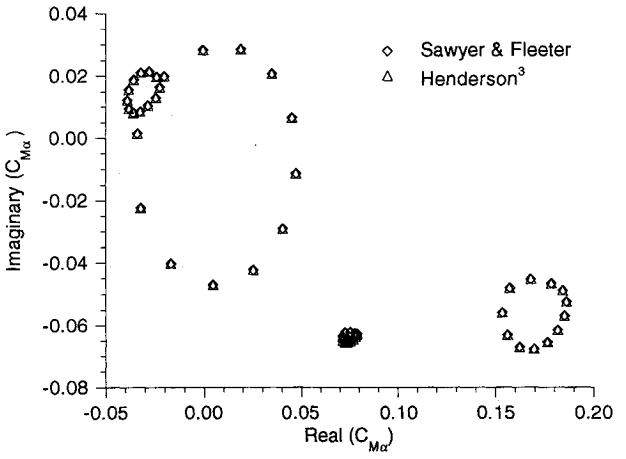

Fig. 7 Aerodynamic model verification for a detuned cascade in torsion.

Figure 6 shows the correlation of the real and imaginary components of the torsion mode moment coefficients from the tuned cascade analysis of Smith and the detuned analysis developed herein. Clearly, there is very good correlation of these predictions.

An incompressible-flow detuned-cascade model was developed by Henderson.[3] The correlation of the incompressible torsion mode moment coefficients and those obtained with the compressible flow model developed herein is obtained by setting the Mach number equal to zero (Fig. 7). In particular, this figure shows this correlation of the real and imaginary components of the influence coefficients for a detuned cascade geometry of $S/c = 2.0$, $C_r = 0.7$, $S_r = 0.4$, $os = 0.2$, $\psi = 45$ deg, $k = 0.8$, and $ea_a = ea_b = 0.5$. All influence coefficients show excellent agreement.

Results

The effect of aerodynamic and structural detuning on flutter is demonstrated by applying the model developed herein to a baseline 12-bladed rotor and detuned variations of this rotor. The baseline tuned cascade depicted in Fig. 8 has a solidity of 1.0, a 45-deg stagger angle, a midchord elastic axis, and a Mach number of 0.5. The mass ratio and the radius of gyration are specified as 193 and 0.4, respectively, values typical of compressor blading.

To demonstrate the effect of aerodynamic and structural detuning on flutter, the baseline tuned cascade must be un-

stable. For a reduced frequency of 0.525, the baseline tuned cascade is unstable in a mode characterized by a detuned interblade phase angle of 120 deg (Fig. 9).

Cascades with full chord airfoils, $C_r = 1.0$, are detuned through the variation of the spacing ratio S_r, the offset os, or the elastic axis location ea_b, from their baseline tuned values.

The effect on stability of aerodynamic detuning associated with changing the spacing ratio of the baseline cascade is shown by considering detuned cascades with spacing ratios of 0.3, 0.4, and 0.6, depicted in Fig. 10. Note that the detuned cascades with spacing ratios of 0.4 and 0.6 are equivalent representations of the same cascade with the upper and lower passages interchanged. The stability of the detuned full chord cascades is presented in Fig. 11. The detuned cascade with a spacing ratio of 0.3 is stable for all modes. However, the detuned cascades with the 0.4–0.6 spacing ratio are unstable for a mode defined by a detuned interblade phase angle of 120 deg.

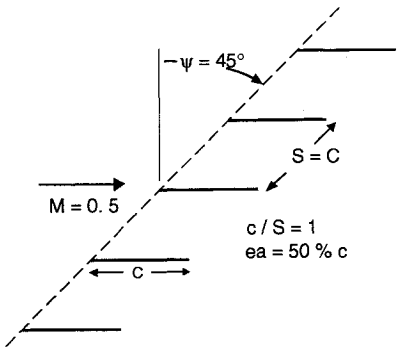

Fig. 8 Baseline tuned cascade.

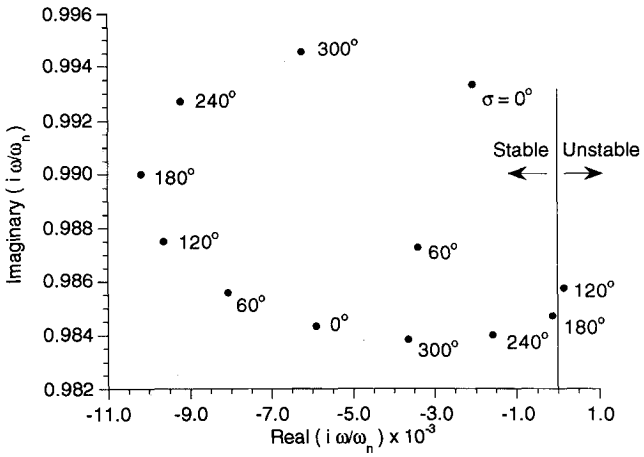

Fig. 9 Stability of baseline cascade.

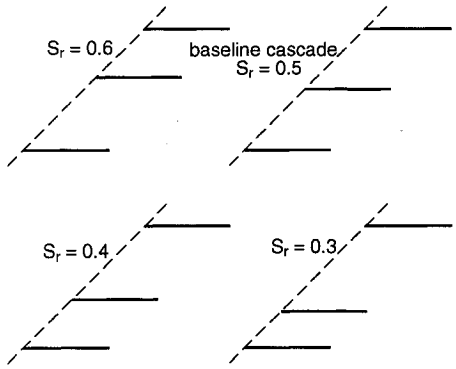

Fig. 10 Detuned cascades with nonuniform circumferential spacing.

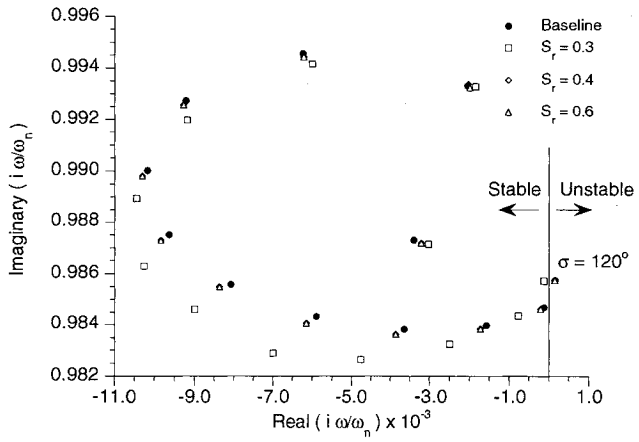

Fig. 11 Stability of detuned cascades with nonuniform circumferential spacing.

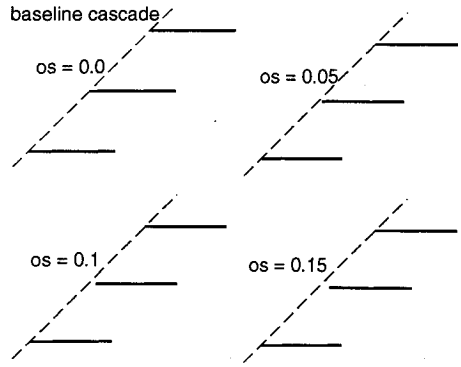

Fig. 12 Detuned cascades with chordwise offset.

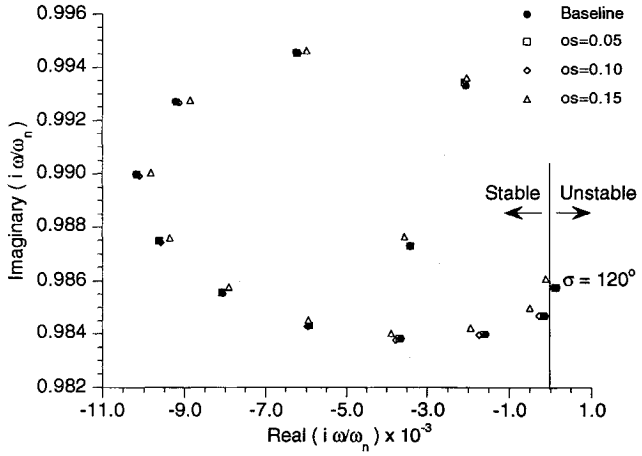

Fig. 13 Stability of detuned cascades with chordwise offset.

Aerodynamic detuning is also incorporated into the baseline cascade by changing the chordwise offset. Detuned cascades with chordwise offset are depicted in Fig. 12. Detuned cascades with offsets of 5, 10, and 15% chord (os = 0.05, 0.10, and 0.15) are considered. The effect on stability of varying the chordwise offset is shown in Fig. 13. Increasing the offset tended to increase the stability of the cascade. The cascades with offsets of 0.05 and 0.10 are unstable for a detuned interblade phase angle of 120 deg. However, further increasing the offset to 0.15c resulted in a stable cascade for all interblade phase angles.

Detuning the baseline cascade by varying the elastic axis location, i.e., detuned cascades with ea_a not equal to ea_b, is schematically depicted in Fig. 14. The effect on stability of detuned cascades with $ea_a = 0.5$ and $ea_b = 0.4$ and 0.6 is

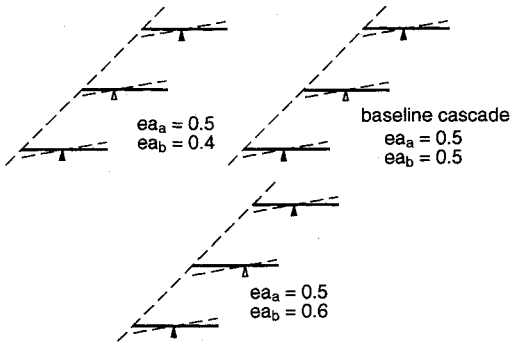

Fig. 14 Detuned cascades with unequal elastic axis locations.

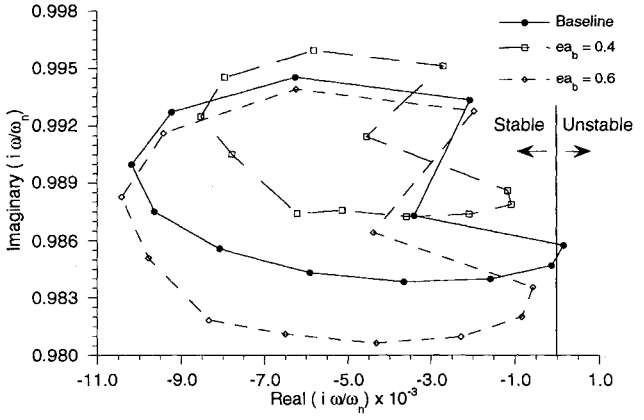

Fig. 15 Stability of detuned cascades with unequal elastic axis locations.

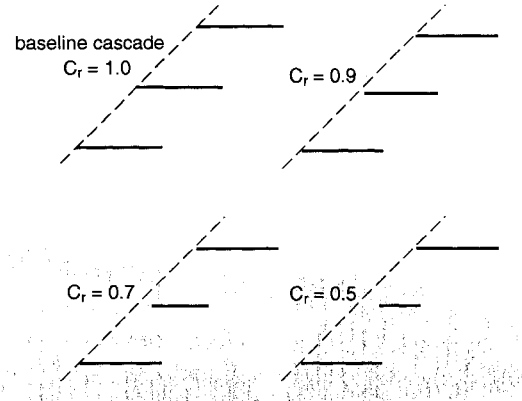

Fig. 16 Detuned cascades with splitter blades.

shown in Fig. 15. Both detuned cascades exhibit increased stability, being stable for all interblade phase angles. The variation of the elastic axis location has a much larger influence on stability than changing either the spacing ratio or the offset.

The effect on stability of detuning the baseline cascade with splitters, i.e., replacing alternate airfoils with splitters, is also considered. In addition to varying the splitter chord length through C_r, which was 1.0 for detuned cascades with full chord airfoils, the spacing ratio, the offset and the elastic axis location of the full chord airfoils or the splitter airfoils are also varied.

The effect on stability of varying the splitter chord length of the detuned cascade is accomplished by considering cascades with splitter chord lengths of 0.9, 0.7, and 0.5, depicted in Fig. 16. The splitters are located at midpassage with the midchord of the splitters and the full chord blades aligned. The effect on stability is shown in Fig. 17. All detuned cascades with splitters are stable, with stability increasing for

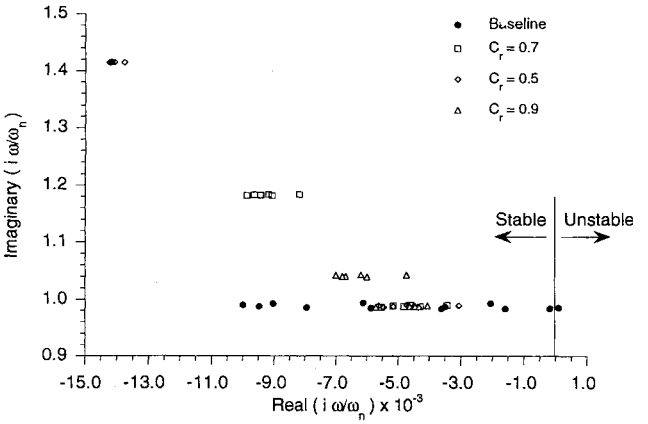

Fig. 17 Stability of detuned cascades with splitter blades.

decreasing chord ratio. Also, note that the splitters oscillate at near their natural frequency, with the splitter natural frequency being the inverse of the square root of the chord ratio ($1/\sqrt{C_r}$).

Summary and Conclusions

A mathematical model has been developed to predict the unsteady aerodynamics of a detuned two-dimensional flat plate cascade in subsonic compressible flow. Aerodynamic detuning was introduced by nonuniform circumferential spacing and also chordwise offset. Combined aerodynamic-structural detuning was accomplished by replacing alternate airfoils with splitter blades.

The effect of aerodynamic and combined aerodynamic-structural detuning on torsion mode stability was demonstrated by combining the unsteady aerodynamic model with a single degree-of-freedom structural model. This flutter stability analysis was then applied to a baseline unstable 12-bladed rotor and detuned variations thereof. Detuned cascades with full chord airfoils and nonuniform circumferential spacing or chordwise offset showed only a small improvement in stability. However, detuned cascades with full chord airfoils and unequal elastic axis locations showed a larger stability improvement. In general, detuned cascades with splitter blades showed great stability improvement. Thus, detuning is a viable passive flutter control technique.

References

[1]Crawley, E. F., and Hall, K. C., "Optimization and Mechanisms of Mistuning of Cascades," American Society of Mechanical Engineers Paper 84-GT-196, 1984.

[2]Chiang, H. D., and Fleeter, S., "Passive Control of Flow Induced Vibrations by Splitter Blades," *Journal of Turbomachinery*, Vol. 116, No. 3, 1994, pp. 489–500.

[3]Henderson, G. H., and Fleeter, S., "Oscillating Aerodynamics and Flutter of an Aerodynamically Detuned Cascade in an Incompressible Flow," *International Journal of Turbo and Jet Engines* (to be published).

[4]Hoyniak, D., and Fleeter, S., "Aerodynamic Detuning Analysis of an Unstalled Supersonic Turbofan Cascade," *Journal of Engineering for Gas Turbines and Power*, Vol. 108, No. 1, 1986, pp. 60–67.

[5]Spara, K. M., and Fleeter, S., "Supersonic Turbomachine Rotor Flutter Control by Aerodynamic Detuning," *Journal of Propulsion and Power*, Vol. 9, No. 4, 1993, pp. 197–206.

[6]Topp, D. A., and Fleeter, S., "Splitter Blades as an Aeroelastic Detuning Mechanism for Unstalled Supersonic Flutter of Turbomachine Rotors," *Journal of Turbomachinery*, Vol. 108, No. 2, 1986, pp. 244–252.

[7]Fleeter, S., Hoyniak, D., and Topp, D. A., "Control of Rotor Aerodynamically Forced Vibrations by Splitters," *Journal of Propulsion and Power*, Vol. 4, No. 5, 1988, pp. 445–451.

[8]Smith, S. N., "Discrete Frequency Sound Generation in Axial Flow Turbomachines," Ames Research Center R&M 3709, March 1972.